The 275 Ma arc-related La Carbonera stock in the northern Oaxacan Complex of southern Mexico: U-Pb geochronology and geochemistry

Luigi A. Solari[1,*], Jaroslav Dostal[2], Fernando Ortega-Gutiérrez[1], and J. Duncan Keppie[1]

[1]*Departamento de Geología Regional, Instituto de Geología, Universidad Nacional Autónoma de México, Ciudad Universitaria, 04510 Del. Coyoacán, México D.F., México*
[2]*Department of Geology, Saint Mary's University, Halifax, N.S. B3H 3C3, Canada*
**solari@servidor.unam.mx*

ABSTRACT

The 300 m wide La Carbonera stock intrudes the northern ~1 Ga Oaxacan Complex, and ranges in composition from diorite through granodiorite to granophyric granite. The associated brecciation of the host rock and the zoned nature of amphibole and plagioclase suggest an explosive mechanism of intrusion. U-Pb analyses of abraded zircons yield variably discordant data that plot on a chord with intercepts at ~1,400 Ma and 275 ± 4 Ma, the latter interpreted as the time of intrusion based on the nearly concordant analysis of euhedral crystals. The upper intercept may be interpreted in terms of a mixed crustal source in the Oaxacan Complex that may include subducted sediments and enriched mantle sources. Variations in the major elements with silica (55->75%) suggest that the rocks represent a consanguineous series with crystallization of amphibole, Fe-Ti oxides and apatite up to ~60% SiO_2, above which plagioclase crystallized. Their chondrite-normalized REE patterns are enriched in LREE, with this enrichment decreasing with increasing SiO_2 content. Their arc magmatic signature is recorded by various chemical discriminants: (1) mantle-normalized trace element patterns which show depletion in Nb and Ti; (2) their locations on Nb+Y versus Rb tectonic discrimination diagram; and (3) their locations in the pre-collisional field in the Batchelor and Bowden's chemical classification scheme. La Carbonera stock appears to form part of the Permo-Triassic magmatic arc that extends from the southern U.S.A through Mexico to Colombia, which has been related to subduction of Pacific plates beneath the western margin of Gondwana.

Keywords: Geochronology, Geochemistry, Oaxacan Complex, La Carbonera stock.

RESUMEN

El intrusivo La Carbonera es un cuerpo de 300 m emplazado en el Complejo Oaxaqueño, y cuya composición varía desde diorita hasta granodiorita y granito granofírico, este último asociado a una brecha compuesta por xenolitos del Complejo Oaxaqueño. La presencia de la brecha, así como el zoneamiento múltiple del anfibol y la plagioclasa sugieren un mecanismo explosivo de la intrusión. Los fechamientos de U-Pb en zircones pulidos dan una discordia cuyas intersecciones son de ~1,400 Ma y de 275 ± 4 Ma, la última interpretada como la edad de cristalización. La intersección superior sugiere la presencia, en el Complejo Oaxaqueño, de una fuente cortical con contribución de sedimentos subducidos y manto enriquecido. La variación de los elementos mayores en contra de SiO_2 sugiere que las rocas constituyen una serie de cristalización consanguínea, con cristalización de anfibol, óxidos de Fe y Ti y apatito hasta ~ 60% SiO_2, arriba del cual cristalizó plagioclasa. Los patrones de tierras raras normalizados con respecto a la condrita C1 muestran un

enriquecimiento en LREE, que disminuye con el aumento del contenido de SiO_2. La firma de arco magmático está confirmada por diferentes variables: 1) empobrecimiento en Ti y Nb en los diagramas de elementos traza normalizados con respecto del manto primitivo; 2) el diagrama de discriminación tectónica de Nb+Y en contra de Rb; 3) la clasificación de Batchelor y Bowden (1985). El intrusivo La Carbonera parece ser parte del arco magmático Permo-Triásico que se extiende desde el sur de Estados Unidos a través de México hasta Colombia, y que ha sido relacionado con la subducción de las placas pacíficas bajo la margen occidental de Gondwana.

Palabras clave: Geocronología, Geoquímica, Complejo Oaxaqueño, intrusivo La Carbonera.

INTRODUCTION

The latest Paleozoic, Mesozoic and Cenozoic geological history of Mexico is dominated by arc magmatism (Sedlock *et al*., 1993). This is easily recognized where the igneous rocks are associated with fossiliferous sedimentary rocks, however, where igneous bodies cut old metamorphic units, their age may only be determined by geochronology. For example, a series of plutons that cut the Acatlán Complex in southern Mexico has been isotopically dated and shown to form part of a Permo-Triassic arc (Torres *et al*., 1999). During mapping of the northern Oaxacan Complex, we encountered a single, small, undeformed, and elliptical stock (300 metres across) that cuts the host gneisses at a high angle along the Highway Cuacnopalan-Tehuacán-Oaxaca, approximately at km 208.5 (N17º18'00'', W97º00'39''), in the State of Oaxaca, southern Mexico (Figure 1). In this paper we present geochemical data to characterize the stock, and the first U-Pb isotopic analyses performed in Mexico at the Laboratorio Universitario de Geoquímica Isotópica (LUGIS), Universidad Nacional Autónoma de México.

FIELD RELATIONSHIPS AND PETROGRAPHY

La Carbonera stock is intrusive into granulitic paragneisses along its steeply dipping western margin. Its eastern contact is a high angle, oblique sinistral-normal, brittle fault. The lithology of La Carbonera stock varies from medium grained, banded quartz-diorite containing a few <20 cm, rounded mafic xenoliths (Figure 2a) in the west (90 m wide), through coarsely crystalline granodiorite (150 m wide), to a breccia (50 m wide) characterized by 80% angular xenoliths of the Oaxacan Complex (<100 cm in size) that may, or may not, be separated by thin fine grained granophyre sheets (Figure 2b). Aplitic veins (<10 cm thick) cut across the diorite, granite and xenoliths.

The quartz diorite is hypidiomorphic with 2-3.5 mm sized hydrous mafic phases set in a quartz-poor, fine-grained feldspar matrix. The mafic phases are mainly zoned hornblende, consisting of alternating brown hornblende and green tremolite, rimmed by deuteric uralite, as well as brown to reddish biotite commonly intergrown with hornblende. Opaque ore minerals appear to be associated with solid-state alteration of the mafic silicates. Accessory minerals include abundant euhedral, short prismatic apatite, zoned allanite, and stubby to rounded zircon. Plagioclase occurs as phenocrysts and in the matrix mixed with quartz. It displays oscillatory zoning, with a composition in the andesine range and is patchily altered to saussurite and epidote. Quartz, which amounts to about 10 % of the rock, fills the irregular spaces between the other magmatic minerals. Deuteric alteration of the mafic minerals produced a complete series of high-low temperature secondary phases: titanomagnetite, uralitic green to bluish green amphibole, epidote/clinozoisite, tremolite/actinolite, green biotite, chlorite, prehnite, sericite, and calcite. Calcite is particularly abundant in some of these rocks, indicating the activity of CO_2-rich fluids towards the end of the deuteric process.

The granodioritic part of the intrusion is rich in biotite, may or may not contain hornblende, and includes some potassium feldspar. In general, this lithology is more strongly altered, with development of abundant epidote/clinozoisite and prehnite at the expense of plagioclase and biotite, respectively. Sulphide is an additional secondary mineral in these rocks. The most distinctive petrographic aspect of the hornblende-free granodioritic rocks is the extreme elongation of zircon (up to 10/1, prisms) and apatite (up to 100/1, needles). Apatite, in particular, is very abundant and commonly forms radial aggregates. Allanite occurs as large, zoned, and strongly coloured euhedral crystals in shades of brown and yellow. The potassium feldspar of these rocks is mainly microcline-perthite commonly with large patches that are still orthoclase or low sanidine. Plagioclase also occurs as strongly zoned phenocrysts with a composition close to sodic oligoclase (based only on its optical properties).

Some of the granitic phases may be considered felsic granophyres because of the development of spectacular micrographic textures formed by eutectoid aggregates of quartz-K-feldspar in a matrix with common albite grains and abundant quartz, microcline and biotite (Figures 3 a and b). Biotite crystallized as semi-radial clusters of extremely thin plates to skeletal crystals (Figure 3b). Accessory phases in these rocks include abundant allanite, apatite, sulphide, titano-

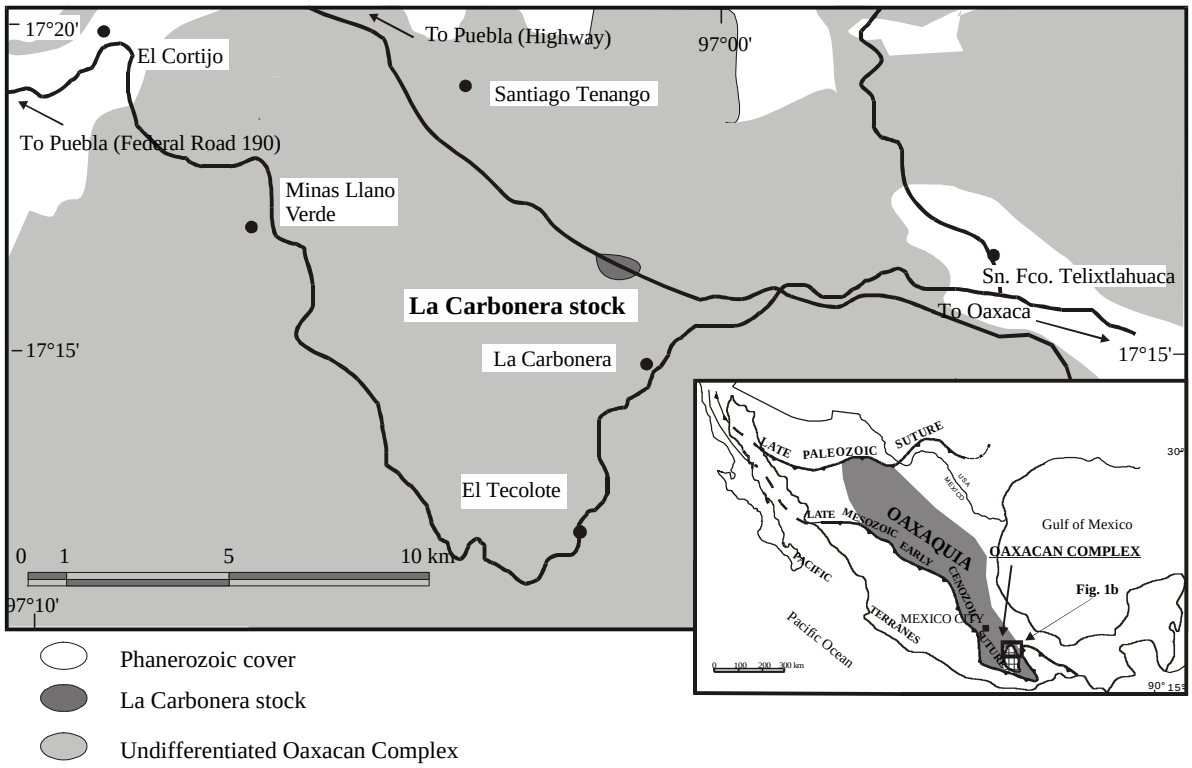

Figure 1. Simplified geological map of the northern Oaxacan Complex showing the location of La Carbonera stock. Inset shows location relative to major terranes of Mexico (modified after Keppie and Ortega, 1995).

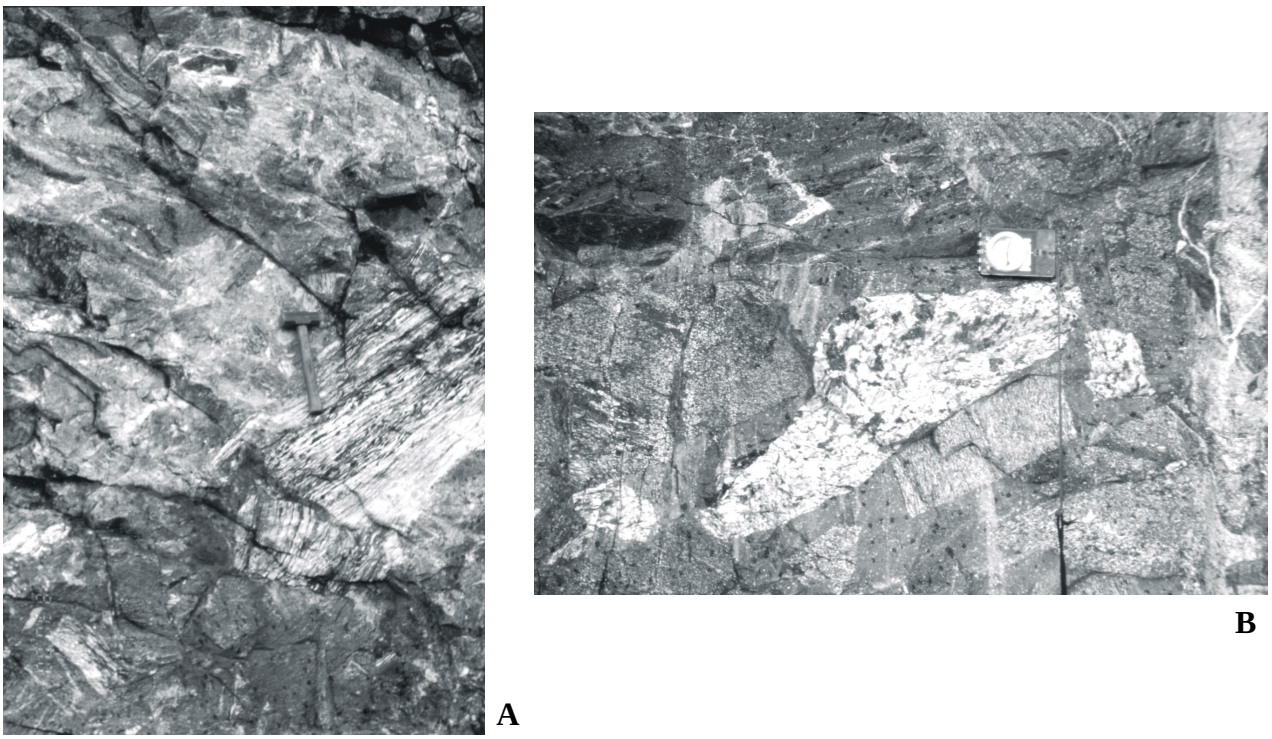

Figure 2. Granulitic xenoliths derived from the Oaxacan Complex in La Carbonera stock: (A) partially assimilated, banded xenolith in the diorite, behind the hammer (30 cm long); (B) angular xenoliths in the breccia. Note the almost complete absence of magma between the large, white xenolith in the middle, and the surrounding other rectangular xenoliths.

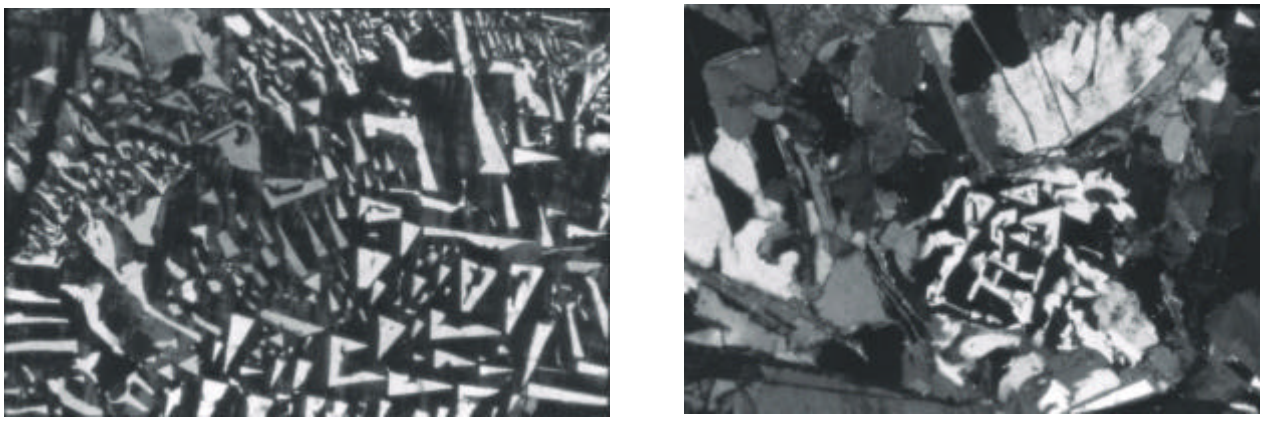

A **B**

Figure 3. Photomicrographs of the granophyric texture taken under crossed polarizers: (A) Detail of the quartz (light grey, triangular to rectangular shape) – K-feldspar (dark grey) intergrowth texture. Width of the picture is 0.5 mm; (B) granophyric texture surrounded by intergrown plagioclase and biotite crystals. Note the skeletal texture of the biotite (thin, elongated crystals roughly oriented NW-SE). Width of the picture is 2.5 mm.

magnetite (probably secondary), zircon, and monazite, whereas deuteric phases include epidote/clinozoisite, chlorite, muscovite, and titanite. Allanite probably precipitated early from the magma because it is euhedral, zoned, and may occur as inclusions in plagioclase phenocrysts. Sporadic garnet is present as xenocrysts in most of the examined rocks. It may be rimmed by kelyphitic coronas of uralite-biotite-epidote, which indicates inheritance from the surrounding mafic gneisses.

From these petrographic and outcrop features of the intrusion, it is tentatively concluded that the body was originally emplaced at high temperatures and apparently along a supercooled path (brown hornblende, acicular apatite and zircon, skeletal biotite), under high water pressures (stability of magmatic hornblende and allanite, intense deuteric alteration at medium to low temperatures), but at relatively shallow depths (miarolitic cavities, granophyric texture). A minimum depth of about 5 km is envisaged for the hornblende-bearing phases in order to allow for the stability of the magmatic amphibole, and for the conversion of potassium feldspar to microcline, which requires a slow cooling rate. Access of magma from greater depths is implied by the presence of dioritic rocks. On the other hand, the strong deuteric alteration indicates the presence of near surface fluids.

The zoned character of the amphibole and feldspar suggests alternations in the physical conditions of crystallization during intrusion. Similar zoned amphiboles occurring in appinites associated with explosion breccias in NW Scotland were attributed to the build up and release of pressure associated with the explosive mechanism of intrusion (Bowes *et al.*, 1964). In view of the competence of the Oaxacan Complex, a similar explosive mechanism is envisaged for La Carbonera stock. The west to east gradation from diorite through granodiorite to granite, and the predominance of the breccias along the eastern margin of La Carbonera stock may be explained in one of two ways. Either La Carbonera stock could have been tilted after intrusion, or the late differentiates could have accumulated near the eastern margin of an irregularly shaped magma chamber.

GEOCHEMISTRY

Fifteen representative samples of La Carbonera stock were analysed by X-ray fluorescence for major and some trace elements (Rb, Sr, Ba, Y, Nb, Zr, V, Cr, Co, Ni, Cu, Zn, Ga) at the Regional Geochemical Center, Saint Mary's University, Halifax, Canada. Precision and accuracy of the X-ray fluorescence technique, as discussed in Dostal *et al.* (1994), are in general better than ± 5% for major elements, and 2-10% for trace elements. Seven samples from this set were selected for the determination of rare-earth elements (REE), Nb, Ta, U and Th with inductively coupled plasma-mass spectrometry (ICP-MS) at the Ontario Geological Survey in Sudbury, Canada. The ICP-MS method, described by Ayer and Davis (1997), indicates a precision and accuracy of < 5-10 %.

Many of the rocks have been affected by secondary processes including deuteric alteration, which may have modified their composition. Thus, the samples were petrographically and chemically screened, and strongly altered samples including those with high LOI values were discarded. The remaining samples are compositionally similar to modern rock suites, and thus, the concentrations of most major elements as well as high-field-strength elements (HFSE), REE and transition elements are thought to reflect the primary magmatic distribution. These samples are employed for petrogenetic considerations and to discriminate the tectonic setting.

The subdivision in three groups of rocks as recognized in the field and by petrography (diorite,

granodiorite and granite) is also reflected in their geochemical signatures. The diorites have SiO_2 ranging from 55 to 62 wt% (LOI-free) (Figure 4). The granodiorites contain 65-73 wt% SiO_2, whereas the granites have > 75 wt% SiO_2 (Table 1). The diorite has about 1-2 wt.% K_2O, granodiorite about 2 wt.%, and granite ~ 3 wt.% K_2O, and the K_2O/Na_2O ratio increasing from ~0.4-0.5 in diorite and granodiorite to about 1 in granite (Figure 4f and h). According to the classification of LeMaitre (1989), the rocks plot in the medium-K field. The rocks show some systematic compositional variations with increasing SiO_2: TiO_2, FeO_{tot}, MgO and P_2O_5 decrease steeply from 55 to 60 wt.% SiO_2, whereas from 60 to 76 wt.% SiO_2, their decrease is gradual (Figure 4a, c, e, and g respectively). In contrast, Al_2O_3 is nearly constant between 55 and 62 wt.% SiO_2, but at the higher SiO_2 values it decreases. The opposite holds true for Na_2O, which initially increases and then remains

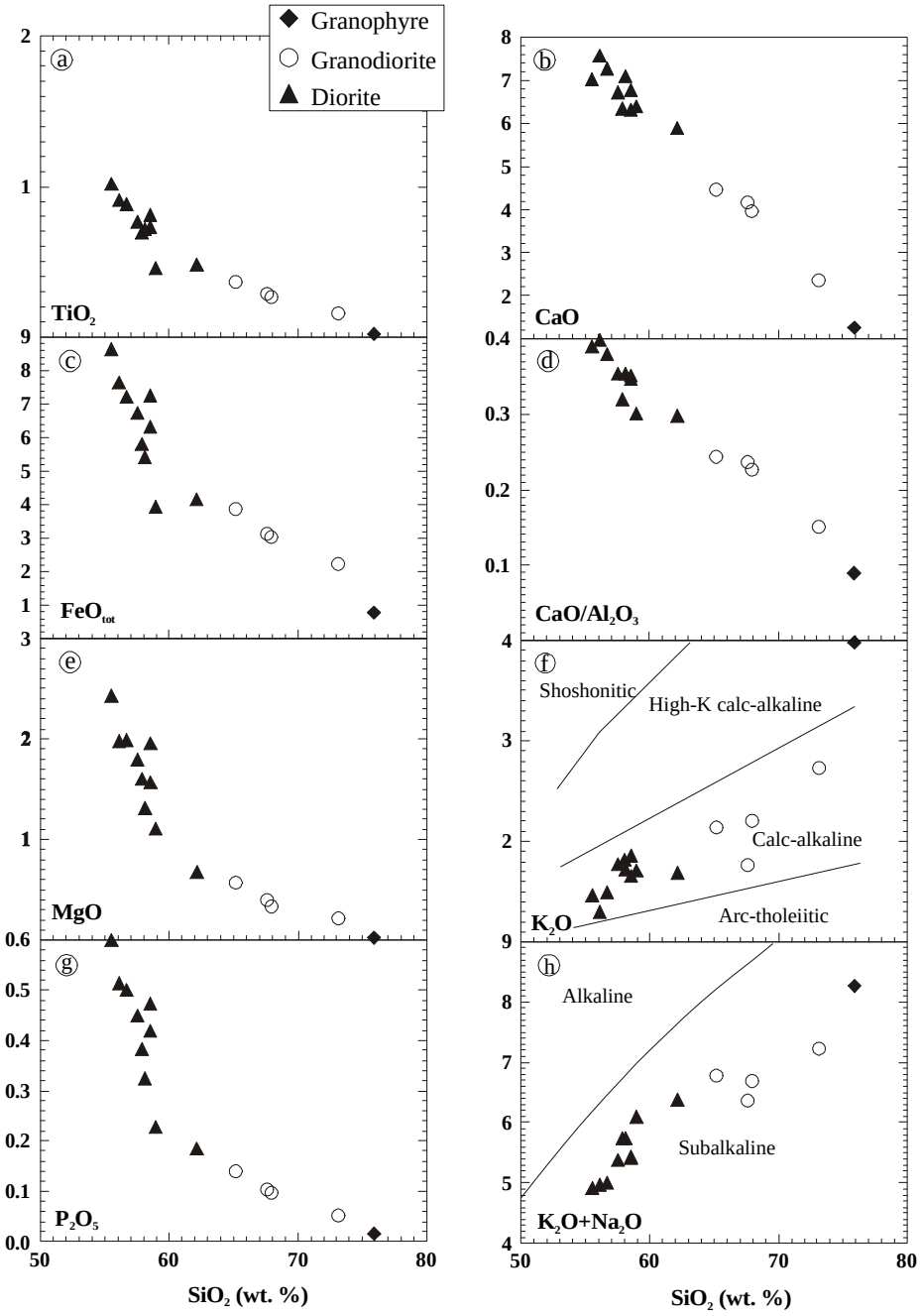

Figure 4. TiO_2 (wt. %), CaO (wt. %), FeO_{tot} (wt. %), CaO/Al_2O_3 (wt. %), MgO (wt. %), K_2O (wt. %), P_2O_5 (wt. %) and K_2O+Na_2O (wt. %) *vs.* SiO_2 (wt. %) diagrams for the analyzed samples of La Carbonera stock. Subdivision fields in the K_2O *vs.* SiO_2 diagram are after Peccerillo and Taylor (1976), whereas alkaline - subalkaline subdivision in the K_2O+Na_2O *vs.* SiO_2 diagram is from Irvine and Baragar (1971).

Table 1. Major and trace element composition of the selected samples of La Carbonera stock. Major element abundances in wt.%.

	Diorites										Granodiorites				Granophyre
Sample	**D-2**	**D-7**	**D-9**	**D-10**	**D-11**	**D-12**	**D-13**	**D-14**	**D-15**	**D-16**	**GD-3**	**GD-4**	**GD-5**	**GD-6**	**G-1**
SiO_2	62.14	58.1	57.6	58.5	58.6	57.9	58.9	56.7	55.6	56.1	65.2	73.2	67.6	68.0	75.9
TiO_2	0.48	0.72	0.770	0.808	0.730	0.694	0.459	0.882	1.018	0.908	0.365	0.157	0.289	0.265	0.022
Al_2O_3	19.71	19.99	18.97	18.17	19.23	19.83	21.31	19.15	18.04	18.97	18.27	15.57	17.64	17.44	14.06
Fe_2O_3*	4.61	5.95	7.39	7.98	6.93	6.38	4.34	7.92	9.58	8.47	4.25	2.43	3.43	3.35	0.85
MnO	0.07	0.08	0.133	0.158	0.130	0.122	0.086	0.149	0.19	0.164	0.061	0.033	0.046	0.034	0.026
MgO	0.68	1.31	1.80	1.96	1.57	1.60	1.11	1.99	2.43	1.98	0.57	0.22	0.4	0.33	0.02
CaO	5.89	7.09	6.72	6.31	6.76	6.35	6.40	7.26	7.03	7.57	4.46	2.35	4.17	3.96	1.25
Na_2O	4.69	4.02	3.61	3.58	3.76	3.98	4.39	3.51	3.45	3.67	4.63	4.49	4.59	4.49	4.29
K_2O	1.69	1.72	1.78	1.86	1.66	1.76	1.71	1.50	1.46	1.3	2.14	2.73	1.77	2.2	3.98
P_2O_5	0.19	0.325	0.450	0.472	0.419	0.383	0.229	0.502	0.599	0.513	0.139	0.053	0.104	0.098	0.015
L.O.I.	0.54	1.07	1.29	1.18	1.12	1.69	1.38	1.00	1.50	1.00	0.58	0.48	0.39	0.69	0.33
Totals	100.14	99.3	99.2	99.8	99.7	99.0	99.0	99.5	99.3	99.7	100.1	101.2	100.0	100.1	100.4
Rb (ppm)	46	43	40	40	39	43	46	31	29	28	55	70	48	52	104
Cs	-	-	-	-	-	0.87	0.68	-	0.72	0.77	0.65	-	0.41	-	1.06
Ba	949	1050	1135	1021	1101	877	892	967	896	659	1288	1610	1579	1371	676
Sr	907	887	756	696	748	738	828	780	697	813	749	530	714	671	121
Ga	26	23	26	22	25	27	26	23	23	23	24	22	24	21	19
Ta	-	-	-	-	-	0.58	0.53	-	0.68	0.62	0.63	-	0.61	-	0.40
Nb	7	10	8	9	8	7.1	5.4	7	9.6	9.5	8.8	7	8	9	6.5
Zr	142	276	163	156	158	161	110	146	153	169	209	178	115	196	69
Y	< 3	6	14	15	11	18	12	12	17	15	7	< 3	< 3	< 3	5
Cr	< 4	< 4	< 4	< 4	< 4	< 4	< 4	< 4	< 4	< 4	< 4	< 4	< 4	< 4	< 4
Ni	< 3	< 3	< 3	< 3	< 3	< 3	< 3	< 3	< 3	< 3	< 3	< 3	< 3	< 3	< 3
Co	9	13	15	18	15	14	8	18	23	21	6	< 5	5	< 5	< 5
V	49	77	85	89	80	77	54	94	108	96	41	25	34	32	11
Cu	12	23	29	29	26	27	13	28	30	28	6	0	23	44	0
Zn	133	130	126	138	124	101	84	128	142	127	132	115	77	62	62
La	-	-	-	-	-	16.75	9.92	-	19.34	17.58	32.55	-	23.12	-	5.82
Ce	-	-	-	-	-	36.52	21.41	-	42.87	34.31	64.40	-	45.80	-	12.95
Pr	-	-	-	-	-	5.02	2.96	-	5.91	4.60	8.51	-	5.59	-	1.80
Nd	-	-	-	-	-	21.69	12.95	-	23.53	20.25	32.08	-	22.04	-	7.56
Sm	-	-	-	-	-	4.85	2.94	-	4.69	4.25	4.99	-	3.93	-	2.08
Eu	-	-	-	-	-	1.93	1.78	-	1.75	1.72	1.66	-	1.44	-	0.38
Gd	-	-	-	-	-	4.12	2.72	-	4.31	3.88	3.22	-	2.65	-	1.59
Tb	-	-	-	-	-	0.60	0.39	-	0.60	0.58	0.35	-	0.30	-	0.21
Dy	-	-	-	-	-	3.31	2.19	-	3.36	2.76	1.46	-	1.13	-	0.94
Ho	-	-	-	-	-	0.62	0.42	-	0.64	0.55	0.23	-	0.16	-	0.16
Er	-	-	-	-	-	1.60	1.08	-	1.61	1.41	0.50	-	0.36	-	0.40
Tm	-	-	-	-	-	0.23	0.15	-	0.22	0.19	0.06	-	0.05	-	0.06
Yb	-	-	-	-	-	1.45	0.96	-	1.42	1.25	0.34	-	0.26	-	0.36
Lu	-	-	-	-	-	0.22	0.16	-	0.23	0.20	0.06	-	0.04	-	0.06
Hf	-	-	-	-	-	1.77	2.02	-	1.72	1.69	6.46	-	4.44	-	3.12
Pb	11	9	10	8	7	7	10	5	8	9	9	10	11	8	14
Th	5	6	5	3	5	1.69	0.98	4	1.36	1.58	3.07	9	2.29	7	2.03
U	-	-	-	-	-	0.62	1.04	-	0.44	0.47	0.96	-	0.66	-	1.46

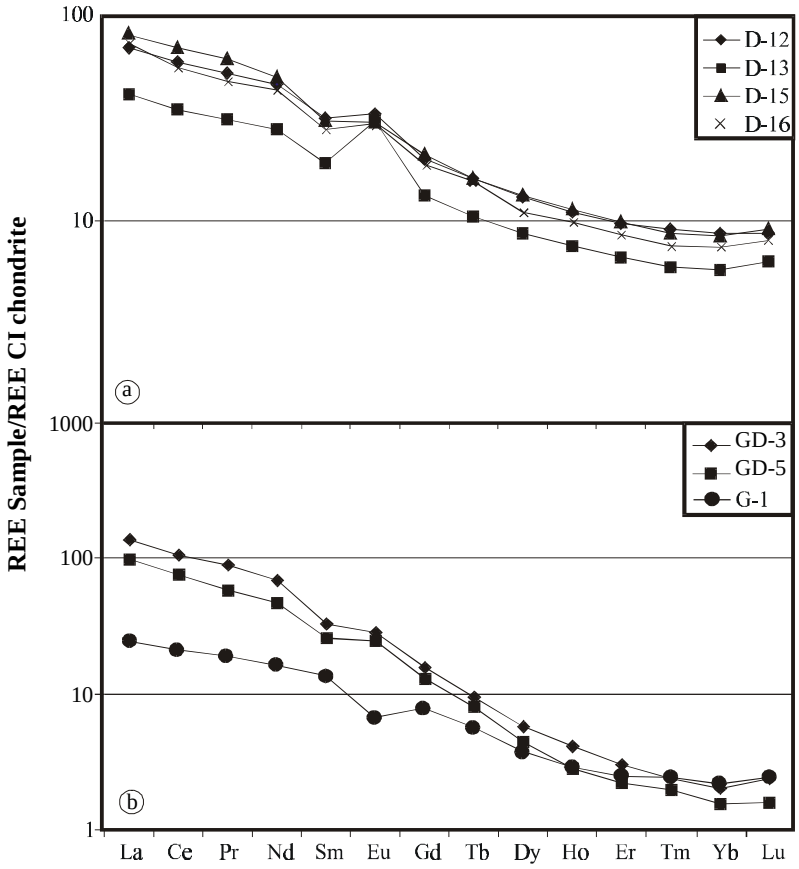

Figure 5. C1 Chondrite – normalized rare earth element diagrams for samples of La Carbonera stock. Normalizing values are from Sun and McDonough (1989). (a) diorite; (b) granodiorite (GD) and granophyric granite (G). Sample numbers as in Table 1.

constant. CaO and CaO/Al_2O_3 decrease with increasing SiO_2 (Figure 4b and d) whereas K_2O and Ba increase. The variation trends suggest that the rocks may represent consanguineous series with crystallization of amphibole, Fe-Ti oxides and apatite up to about 60 wt.% SiO_2. Subsequently the minerals were accompanied by crystallization of plagioclase.

The chondrite-normalized REE patterns (Figure 5) of the diorite show enriched light REE with $(La)_n$ ~30-60 and $(La/Yb)_n$ ~5-10 with variably positive Eu anomalies, the size of which correlate with Al_2O_3 contents suggesting accumulation of feldspars in these rocks. Granodiorites have higher contents of REE and more fractionated patterns with $(La)_n$ ~70-100 and $(La/Yb)_n$ ~55-60. On the other hand, the granites have the lowest REE contents accompanied by $(La)_n$ ~8 and $(La/Yb)_n$ ~10 and negative Eu anomaly implying crystallization of feldspar and accessory phases high in REE. All the REE patterns display a concave downward shape of heavy REE with the lowest normalized values for Yb, characteristic of a role of amphibole in the rock evolution. The mantle normalized trace element patterns of all the rocks (Figure 6) show depletion in Nb and Ti, typical of subduction-related or crustally derived magmas. An arc tectonic setting is also indicated by Rb *vs.* Y+Nb plot (Figure 7). According to chemical classification of Batchelor and Bowden (1985) the rocks are pre-collisional (Figure 8).

U-PB GEOCHRONOLOGY

This paper includes the first U-Pb geochronology analyses performed at LUGIS, UNAM. The analytical procedures will thus described here in detail.

Zircon separation

A medium grained granodiorite sample (Carb 01-99) was selected for zircon dating. About 20 kg of whole rock were crushed with a jaw crusher to ~0.5 cm size, and the crushed material further ground to <500 μm with a Bico© disk grinder. The heavy minerals were concentrated using a Wifley table, from which about 1 kg of material was recovered. This heavy concentrate was further processed with a L1 Frantz© isodynamic magnetic separator with increasing currents up to 1.7 Amps, a side tilt of 10º and a front slope of 15 to 20º. The technique is similar to the one proposed by Krogh

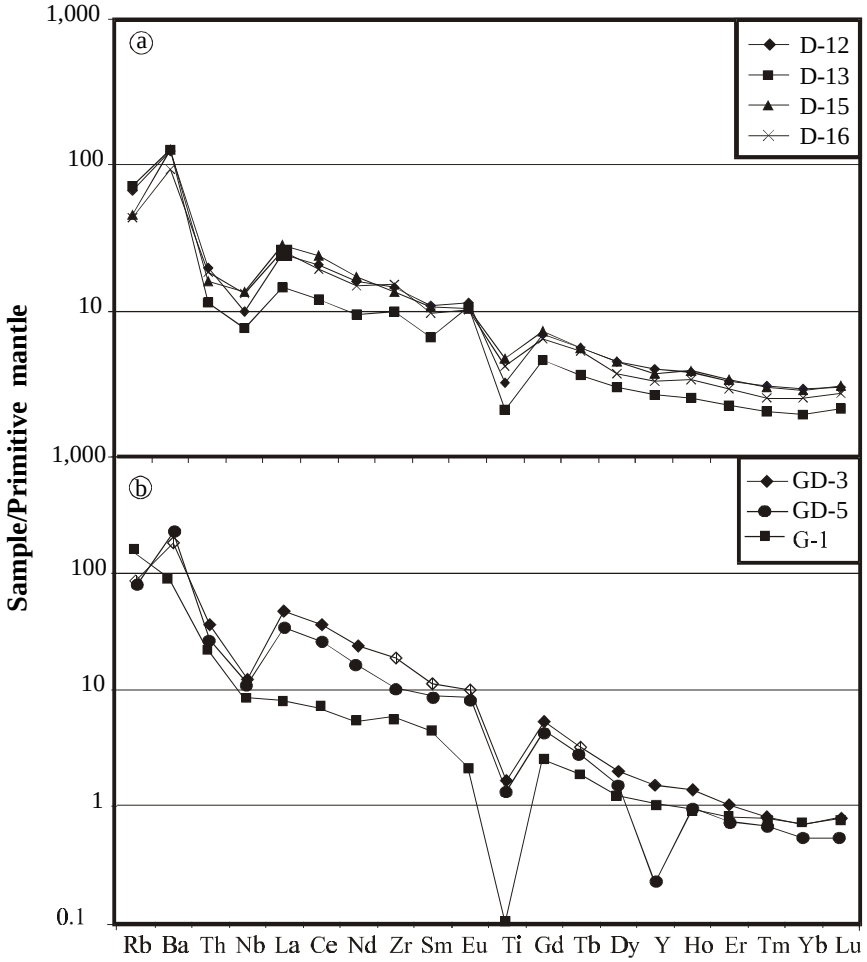

Figure 6. Primitive mantle – normalized incompatible element diagrams for the rocks of La Carbonera stock. Normalizing values are from Sun and McDonough (1989). (a) diorite; (b) granodiorite /GD) and granophyric granite (G). Sample numbers as in Table 1.

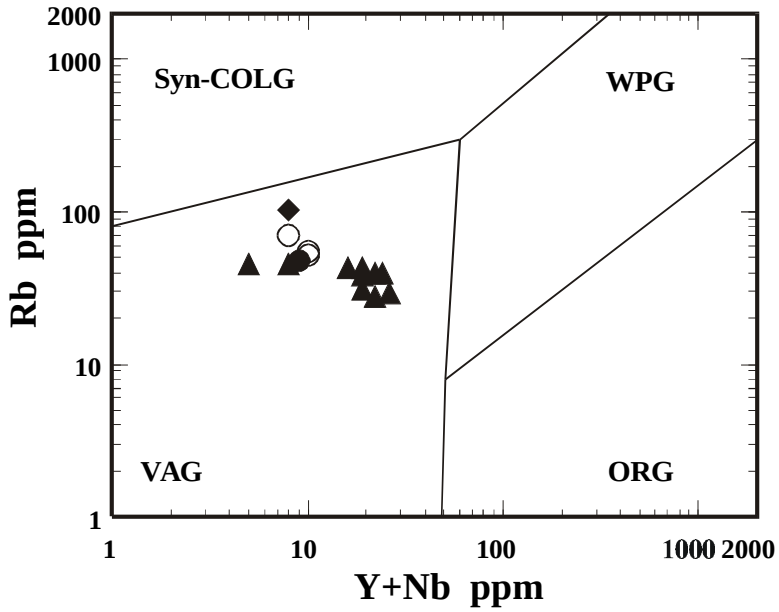

Figure 7. Rb vs. Y+Nb tectonic discrimination diagram for the studied samples of La Carbonera stock. Discrimination diagram is from Pearce *et al.* (1984). Symbols are as in Figures 3 and 8. Fields are: Syn COLG: syn-collisional granites; VAG: volcanic arc granites; WPG: within plate granites; ORG: ocean ridge granites.

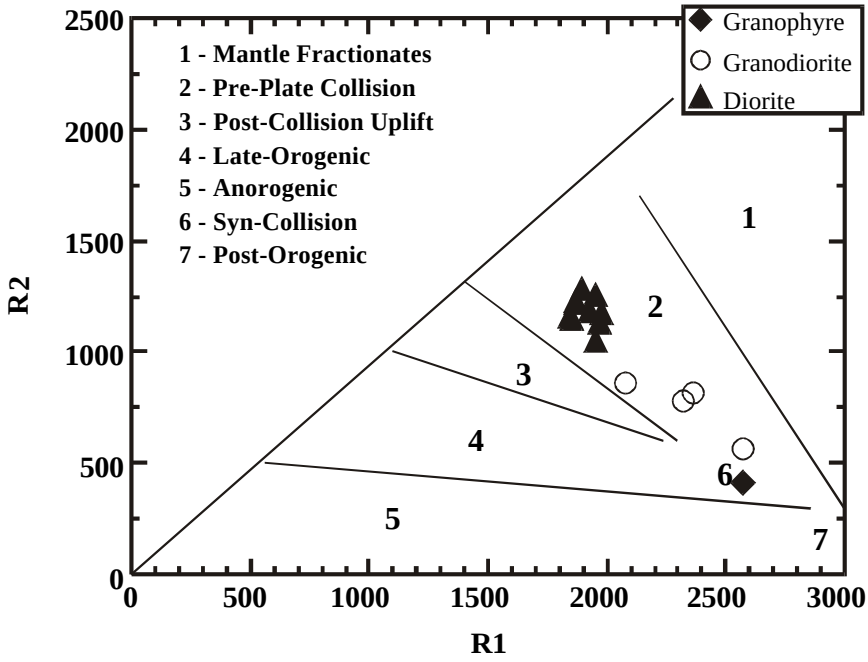

Figure 8. R1-R2 tectonic discrimination diagram from Batchelor and Bowden (1985). R1 is equal to 4Si-11(Na+K)-2(Fe+Ti), whereas R2 is equal to 6Ca+2Mg+Al, with all the cations expressed as millications per 100 g.

(1982b) with minor modifications. The zircons are nonmagnetic, thus the best crystals are in the least magnetic fraction. The nonmagnetic fraction collected at 1.7 Amps was again processed at 1.7 Amps, now decreasing the front slope to 10º and the side tilt from 10° to 7°, 4°, 1°, 0° and –1º in decreasing steps. In this way the nonmagnetic minerals that often accompany zircons in the last concentrate, such as feldspars, sulphides, and some apatites are generally eliminated as well as those zircons with impurities and small inclusions. Heavy liquids were used to further purify the final zircon concentrate. The first heavy liquid used was sodium polytungstate, with a density of about 2.8 g/cm^3. In this way, quartz and feldspars are generally removed. Finally, one pass through methylene iodide (density ~3.35 g/cm^3) ensures the elimination of apatite, and normally yields a concentrate of ~90% zircons.

Zircon description

The analyzed zircon fractions were handpicked in alcohol under binocular microscope using factors such as shape, color, absence of fractures, stain, and any visible core. Large zircons (>150 μm) were preferred, because they generally have a higher volume/surface area ratio and so are less affected by recent lead loss than small ones. Four fractions were chosen for U-Pb geochronology. Fraction 1 was composed of about 40 prismatic grains, with bipyramidal terminations, clear to pale pink colored, 200-300 μm in size with an aspect ratio of up to 4:1. Fraction 2 was made up of 30 bipyramidal, transparent crystals, > 200 μm in size with a similar aspect ratio to fraction 1. Fraction 3 was comprised of about 50 broken pyramids, 80-100 μm in size, whereas fraction 4 consisted of 30 stubby, euhedral and multifaceted grains, up to 150 μm in size. Cathodoluminescence imaging of some of the bigger zircons, with morphologies similar to those of fractions 1, 2 and 3, was also performed to evidence the internal zoning and aid the age interpretations. Imaging was realized at the Instituto de Geología, UNAM, using a Nuclide ELM-3R luminoscope connected to a petrographic microscope.

Crystal polishing and analytical techniques

To decrease potential surficial Pb loss, zircon populations were abraded using an abrader built at LUGIS similar to the one described by Krogh (1982a). A disposable 30 μm screen was used to hold the grains in the abrader. Abrasion was performed at ~ 4 psi for about 6 hours, followed by 2 hours at ~ 1.5 psi for the final polishing. Gem quality pyrite grains were used as abrasive, to which twice the number of similar-sized zircon grains were added . The abraded zircons are oval to rounded in shape, and the small dark spots on the surface were normally removed by washing in warm 4N HNO_3 for about 30 minutes. This final cleaning is important because common Pb in pyrite could significantly in-

crease the analytical blanks. The next steps were performed in the ultra pure area of the LUGIS, using the laboratory internal procedures as follows. Selected zircons were weighed on a microbalance with a precision of ± 1 μg, and put in Teflon Parrish-type microcapsules for digestion (Parrish, 1987). Final cleaning was done by heating in ~0.5 ml ultrapure 6N HCl for 20 minutes on a hot plate, followed by Milli-Q water and 8N HNO_3 rinsing, and final heating for 15 minutes in 8N HNO_3. Digestion was performed by adding to the microcapsule ~0.5 ml of concentrated (48% vol.) HF, and 1 drop of 16N HNO_3. Ultrapure reagents (HF, HNO_3, and HCl) were prepared by distilling Baker© reagent-grade acids at sub-boiling temperature in Teflon bottles. The distiller system used at LUGIS is similar to the one described by Mattinson (1972). Lead blanks, after 6 times distillation, are ~ 3 pg/ml, ~2 pg/ml and ~ 3 pg/ml, respectively.

Microcapsules were placed in a bigger Teflon liner within a Parr® type steel vessel, which was tightly closed and put inside an oven at 220ºC for 5 days to ensure complete digestion of zircons. 0.5 to 5 ml of concentrated HF were added to the Teflon liners, to equilibrate pressure in and out of the microcapsules.

After digestion, microcapsules were carefully extracted, rinsed and put overnight on a hot plate, to dry. The dissolved sample was finally collected in 3.1N HCl, split in IC aliquot (isotopic concentration) and ID aliquot (isotopic dilution) and carefully weighed. The ID aliquot was spiked with ~0.04 ml of West Coast $^{208}Pb/^{235}U$ mixed spike solution and, once capped, left overnight on the hot plate to equilibrate. Column chemistry was performed to separate U and Pb from the samples, for both IC and ID aliquots. Columns were prepared using Zeuss Inc.® heat shrink Teflon, which have a 150 μl reservoir filled with ultraclean BioRad® AG1X8 Chloride form 100-200 mesh anionic resin. Column procedure follows that proposed by Krogh (1973) and Roddick *et al.* (1987) with minor modifications. Pb was collected in 800 μl of 6N HCl, whereas U in 1.5 ml of Milli-Q water in rigorously cleaned Teflon beakers. Spiked U and Pb ID splits were collected together. One drop of 0.1M H_3PO_4 is added to both U and Pb cuts, and they are evaporated on a hot plate at ~90º. IC Pb and ID U and Pb are then loaded separately on Re filament using 1 μl 0.1M H_3PO_4 and 1 μl of clean Silica Gel. Silica Gel - orthophosphoric acid loading technique followed the principles first proposed by Cameron *et al.* (1969). Loading blanks average 3 pg, calculated measuring the $^{208}Pb/^{235}U$ spike loading. Isotopic ratios were determined on a Finnigan® Mat 262 multicollector mass spectrometer, equipped with a second electron multiplier (SEM) – ion counting system to detect lower peaks, such as ^{204}Pb. ^{206}Pb, ^{207}Pb and ^{208}Pb were measured on Faraday collectors. Faraday/SEM counter gains were stable throughout the analysis of one turret (magazine) with an error of 0.01%. Performance is normally checked by repeated analyses of the National Bureau of Standard (now NIST) SRM 983, whereas corrections of mass fractionation were done with simultaneous runs of the SRM 981 Pb and U500 U standard solutions. These indicate a fractionation of 0.12±0.04% a.m.u.$^{-1}$ for Pb isotopic ratios, and 0.12±0.05% a.m.u.$^{-1}$ for U isotopic ratios, values that have been applied to correct the raw isotopic ratios. Common Pb blanks for zircon analyses ranged between 33 and 220 pg, with an average of less than 90 pg. Errors on the zircon analyses were calculated using the program PbDat (Ludwig, 1991), and isochron plot is from the software Isoplot (Ludwig, 1999).

RESULTS AND DISCUSSION

The U-Pb isotopic data of the four abraded zircon fractions are given in Table 2. The low U amount in the zircons (between 11 and 115 ppm) complicates the isotopic determinations because the Pb produced by radiogenic decay is low, and thus isotopic ratios, such as $^{206}Pb/^{204}Pb$ may be very low. This, combined with the common Pb blank that currently ranges between 40 and 220 pg (calculated as sum of reagents, digestion, column chemistry, air and loading blank) results in the high errors recorded in some of the analyzed zircon fractions (*i.e.*, 1 and 2 in Table 2).

All fractions yielded discordant ages between 7 and 41%. Fraction 4 is nearly concordant and has similar $^{206}Pb/^{238}U$ and $^{207}Pb/^{235}U$ ages (279 to 281 Ma). Zircons composing fraction 4 are euhedral, uncoloured, with sharp edges between the facets, and they lack any visible core under the binocular microscope, features indicative of igneous crystallization. A chord through the data yielded intercepts at 275 ± 4 Ma, and ~1400 Ma (Figure 9). Based upon the crystal morphology and the near concordance of fraction 4, the lower intercept is interpreted as the time of intrusion. The upper intercept age of 1,395+180/-200 Ma is similar to the T_{DM} ages currently available in Oaxaquia that range between 1.35 and 1.6 Ga (Ruiz *et al.*, 1988; Lawlor *et al.*, 1999; Weber and Köhler, 2000). Nd isotopic compositions are usually attributed to a variety of sources including subducted sediment, enriched mantle, and crustal assimilation. Although most protolith ages in the Oaxacan Complex range fom 1-1.25 Ga, the paleosome of the El Catrín migmatite yielded an upper intercept age of ~1.4 Ga (Solari *et al.*, 1998), which may represent an exposed remnant of the Oaxacan lowermost crust. Thus, the ~1.4 Ga upper intercept is explicable in terms of crustal assimilation of a mixture of mainly 1.4 Ga lowermost Oaxacan crust, with little contribution from the 1 to 1.25 Ga rocks. This conclusion is supported by the ubiquitous presence of garnet xenocrysts and the abundance of strongly assimilated fragments, belonging to the local gneisses, in La Carbonera stock. However, its arc signature allows the possibility that the source could also include subducted sediments and enriched mantle.

The small apparent differences in the An content of plagioclase and relatively narrow widths of its oscilla-

Table 2. U-Pb geochronology of the Carbonera Stock, southern Mexico.

La Carbonera intrusive, sample Carb 9901

Fraction‡	Weight (mg)	U (ppm)	Total Pb (ppm)	Com. Pb (pg)	$^{206}Pb/^{204}Pb$	$^{207}Pb/^{206}Pb$	$^{208}Pb/^{206}Pb$	$^{206}Pb/^{238}U$	$^{207}Pb/^{235}U$	$^{207}Pb/^{206}Pb$	$^{206}Pb/^{238}U$	$^{207}Pb/^{235}U$	$^{207}Pb/^{206}Pb$	% Disc.
					Observed Ratios†			Atomic Ratios††			Age (Ma)†††			
OC9805-1 prsm, clear, abr	0.2	11	1.2	61	77	0.0882	0.0130	0.06113	0.51656	0.06128	383	423	649±150	41
OC9805-2 byp, abr	0.1	115	5.8	40	162	0.0087	0.0062	0.04538	0.34301	0.05483	286	299	405±130	29
OC9805-3 broken pira-mids, abr	0.25	93	8.7	710	84	0.0108	0.0119	0.04933	0.39329	0.05782	310	337	523±47	41
OC9805-4 stubby, abr, 30 grns	0.28	56	2.4	4	1247	0.0178	0.0008	0.04422	0.31908	0.05233	279	281	300±18	7

Zircon sample dissolution and ion exchange chemistry modified after Krogh (1973) and Mattinson (1987) in Parrish (1987) -type microcapsules. ‡ All non-magnetic fractions at 1.7 Amp. prsm= prismatic grains; byp= bypiramidal; abr= abraded grains. † Observed isotopic ratios are corrected for mass fractionation of 0.12% for ^{208}Pb spiked fraction. Two sigma uncertainties on the $^{207}Pb/^{206}Pb$ and $^{208}Pb/^{206}Pb$ ratios are < 0.4%, generally better than 0.2%; uncertainties in the $^{206}Pb/^{204}Pb$ ratio vary from 0.14% to 0.8%. †† Decay constants used: $^{238}U = 1.55125 \times 10^{-10}\ a^{-1}$; $^{235}U = 9.48485 \times 10^{-10}\ a^{-1}$; $^{238}U/^{235}U = 137.88$. Uncertainities on the U/Pb ratio is 0.5%. ††† $^{207}Pb/^{206}Pb$ age uncertainties are ±2 sigma calculated from the data reduction program PBDAT of K. Ludwig (1991). Total processing Pb blank amount varied between 40 pg and 220 pg. Initial Pb composition are from isotopic analyses of feldspar separates. Isotopic data were measured on a Finnigan MAT 262 mass Spectrometer with SEM Ion Counting at LUGIS, UNAM, Mexico City

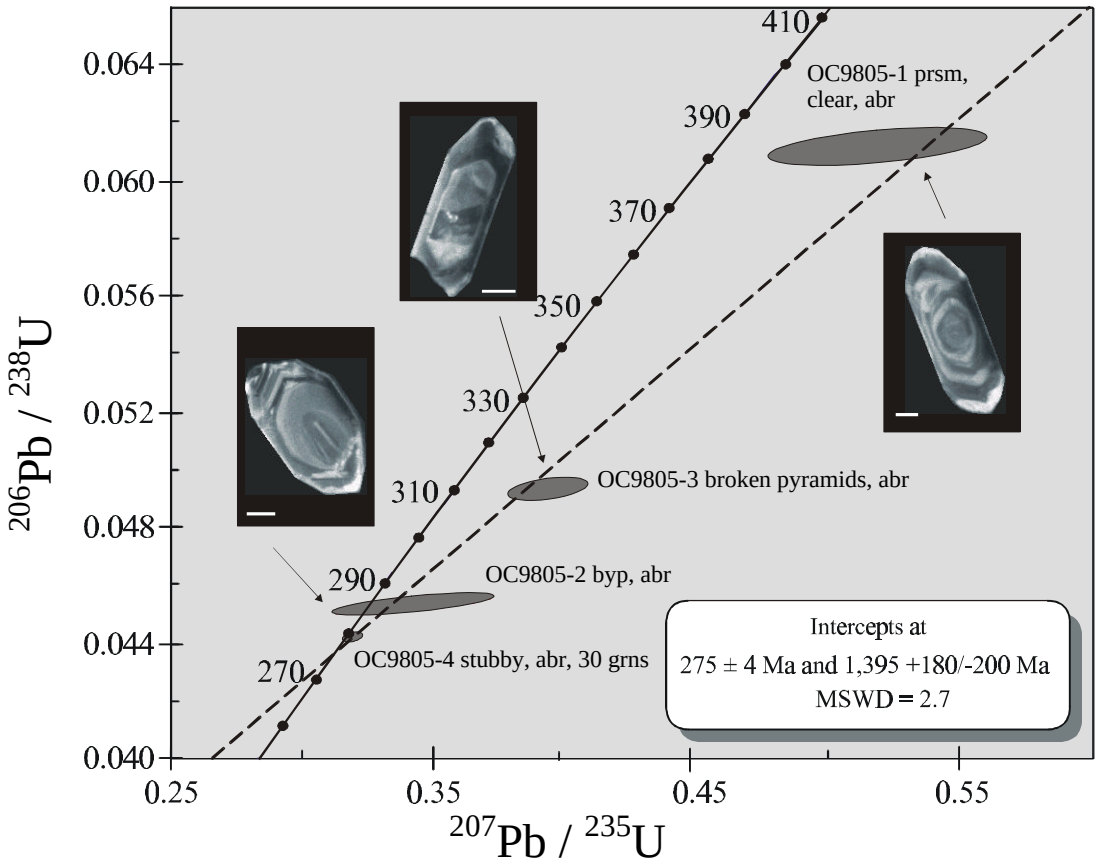

Figure 9. U-Pb concordia diagram for the granodiorite sample of La Carbonera stock. Lower intercept at 275 ± 4 Ma is interpreted as the crystallization age of La Carbonera stock. Insets show CL images for zircons with similar morphologies to the analysed crystals of fractions 1, 2, and 3. Note the presence, in all the imaged grains, of inherited cores entrained in La Carbonera magma. White bar in CL images is 50 μm scale.

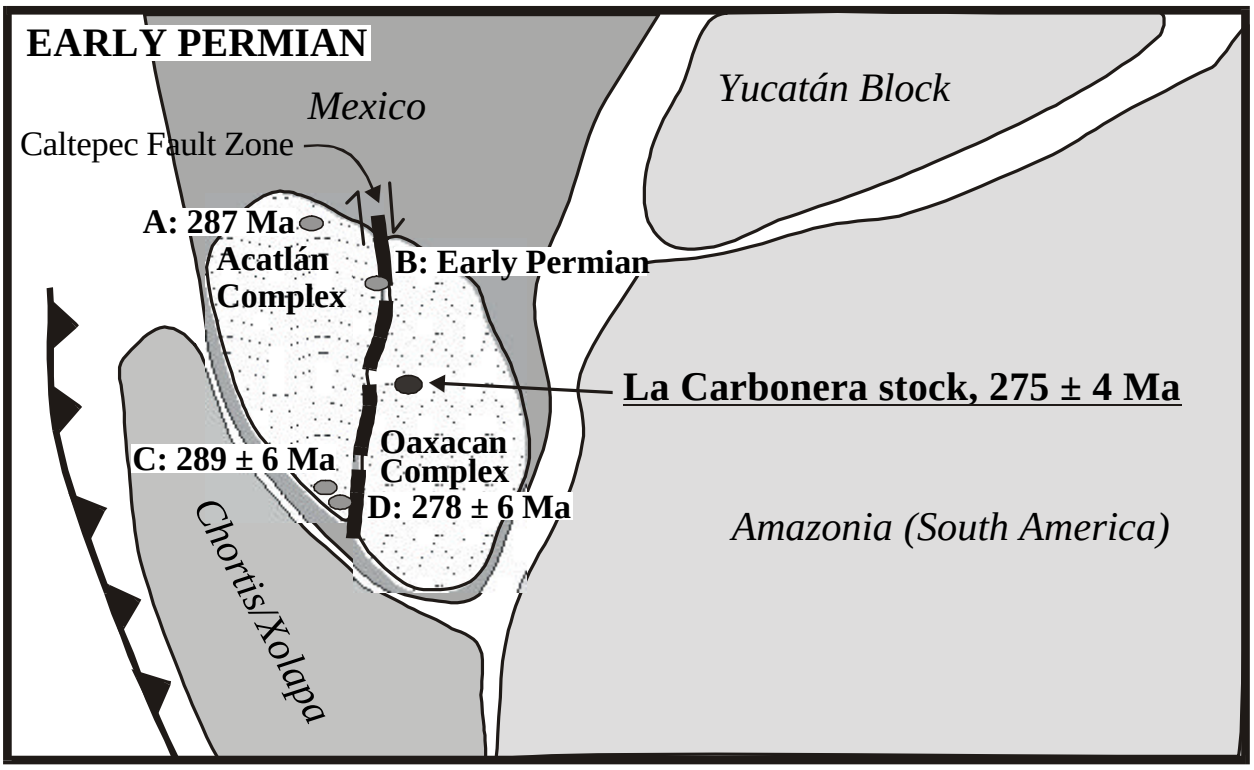

Figure 10. Tectonic model for the evolution of southern Mexico during the Early Permian. Modified from Grajales-Nishimura *et al.* (2000). Reported Early Permian intrusives are: A, Totoltepec stock, 287 Ma (U-Pb on concordant zircons, Yañez *et al*., 1991). B, Cozahuico granite, 269 ± 21 Ma (Rb-Sr isochron, Ruíz-Castellanos, 1979), and Early Permian (U-Pb on zircons, Elías-Herrera and Ortega-Gutiérrez, 2000). C, Juchatengo gabbros, 289 ± 6 Ma (K-Ar on hornblende), and D, Juchatengo granitoids, 282 ± 6 Ma (K-Ar on hornblende), and 282 ± 6 Ma (K-Ar on biotite) (Grajales-Nishimura, 1988).

tory bands may be interpreted in terms of: (1) "near equilibrium incremental diffusion controlled growth" process, most probably in a closed system not associated with mixing of two different magmas; and (2) intermittent explosive intrusion, both of which are common in modern volcanic rocks with oscillatory zoned plagioclase showing substantial changes in An contents and broader bands (Tepley *et al.*, 2000).

CONCLUSIONS

Geochemical and isotopic analyses presented in this paper show that La Carbonera stock is a calcalkaline diorite to granite of Early Permian (~ 275 Ma) age. Similar calcalkaline plutons are widespread in southern Mexico, ranging from ~270 to 290 Ma, where they intrude the lower Paleozoic Acatlán Complex and ~1Ga Oaxacan Complex (Figure 10) (Ruiz-Castellanos, 1979; Ortega-Gutiérrez, 1981; Grajales-Nishimura, 1988; Yáñez *et al*., 1991; Elías-Herrera and Ortega-Gutiérrez, 2000). They have been interpreted as part of a Permo-Triassic continental arc that extended from southern U.S. to Colombia, related to the eastward subduction of the Pacific plate (Torres *et al*., 1999). Thus, it would appear that La Carbonera stock represents part of this magmatic arc.

The U-Pb geochronology of La Carbonera stock is the first report of a zircon dating performed entirely at LUGIS, UNAM. The analytical work reported in this paper can be further improved by decreasing Pb blanks, processing smaller fractions and using a $^{205}Pb/^{235}U$ tracer, which is presently not available.

ACKNOWLEDGEMENTS

We would like to thank several people contributed to this paper: Carlos Ortega helped with zircon separation and handpicking; Consuelo Macías supervised the CL imaging; Gabriela Solís assisted with the LUGIS analytical work, and Juan Julio Morales performed the TIMS determinations. Robert Lopez greatly helped in establishing U-Pb technique at LUGIS, UNAM. Funds for the project were provided by PAPIIT-DGAPA Grants IN136999 (JDK) and IN107999 (FOG), CONACyT grant 25795-T (JDK and FOG), NSERC grant (JD), and PAEP-UNAM Student Grant 205313 (LAS) supported the research. Reviews of P. Shaaf and K. L. Cameron substantially improved the manuscript.

BIBLIOGRAPHIC REFERENCES

Ayer, J.A., Davis, D.W., 1997, Neoarchean evolution of differing convergent margin assemblages in the Wabigoon Subprovince: geochemical and geochronological evidence from the Lake of the Woods greenstone belt, Superior Province, Northwestern Ontario: Precambrian Research: 81, 155-178.

Batchelor, R. A., Bowden, P., 1985, Petrogenetic interpretation of granitic rock series using multicationic parameters: Chemical Geology, 48, 43-55.

Bowes, D. R., Kinloch, E. D., Wright, A. E., 1964, Rhythmic amphibole overgrowths in appinites associated with explosion breccias in Argyll: Mineralogical Magazine, 33-266, 963-973.

Cameron, A.E., Smith, D.H., Walker, R.L., 1969, Mass spectrometry of nanogram-size samples of lead: Analytical Chemistry, 41(3), 525-526.

Dostal, J., Dupuy, C. Caby, R., 1994, Geochemistry of the Neoproterozoic Tilemsi belt of Ilforas (Mali, Sahara); a crustal section of an oceanic island arc: Precambrian Research, 65, 55-69.

Elías-Herrera, M., Ortega-Gutiérrez, F., 2000, Roots of the Caltepec fault zone, southern Mexico–Early Permian epidote bearing anatexitic granitoids: Unión Geofísica Mexicana, 2a. Reunión Nacional de Ciencias de la Tierra. GEOS, Puerto Vallarta, Jal., p. 323 (abstract).

Grajales-Nishimura, J.M., 1988. Geology, geochronology, geochemistry and tectonic implications of the Juchatengo green rock sequence, State of Oaxaca, southern Mexico: Tucson, Arizona, University of Arizona, M. Sc. Thesis, 145 p.

Grajales-Nishimura, J.M., Centeno-García, E., Keppie, J. D., Dostal, J., 2000, Geochemistry of Paleozoic basalts from the Juchatengo complex of southern Mexico–tectonic implications: Journal of South American Earth Sciences, 12, 537-544.

Keppie, J.D., Ortega-Gutiérrez, F., 1995, Provenance of Mexican Terranes–isotopic constraints: International Geology Review, 37, 813-824.

Krogh, T.E., 1973. A low-contamination method for hydrothermal decomposition of zircon and extraction of U and Pb for isotopic age determinations. Geochimica et Cosmochimica Acta, 37, 485-494.

Krogh, T.E., 1982a, Improved accuracy of U-Pb zircon ages by the creation of more concordant systems using an air abrasion technique: Geochimica et Cosmochimica Acta, 46, 637-649.

Krogh, T.E., 1982b, Improved accuracy of U-Pb zircon dating by selection of more concordant fractions using a high gradient magnetic separation technique. Geochimica et Cosmochimica Acta, 46, 631-635.

Lawlor, P.J., Ortega-Gutiérrez, F., Cameron, K.L., Ochoa-Camarillo, H., Lopez, R., Sampson, D.E., 1999, U-Pb geochronology, geochemistry, and provenance of the Grenvillian Huiznopala Gneiss of Eastern Mexico: Precambrian Research, 94(1-2), 73-99.

LeMaitre, R.W., 1989, A classification of igneous rocks and glossary of terms: Oxford, Blackwell, 193 pp.

Irvine, T. N. Baragar, W. R. A., 1971, A guide to the chemical classification of the common volcanic rocks: Canadian Journal of Earth Sciences, 8, 523-548.

Ludwig, K.R., 1991, PbDat–A Computer Program for Processing Pb-U-Th Isotope Data, Version 1.24 88-542: Reston, Va., U.S. Geological Survey.

Ludwig, K.R., 1999, Isoplot/Ex, ver. 2.49, a geochronological toolkit for Microsoft Excel: Berkeley, California Geochronology Center.

Mattinson, J.M., 1972, Preparation of Hydrofluoric, Hydrochloric, and Nitric Acids at ultralow lead levels: Analytical Chemistry, 44(9), 1,715-1,716.

Ortega-Gutiérrez, F., 1981, Metamorphic belts of southern Mexico and their tectonic significance: Geofísica Internacional, 20(3), 177-202.

Parrish, R.R., 1987, An improved micro-capsule for zircon dissolution in U-Pb geochronology: Chemical Geology, 66, 99-102.

Pearce, J.A., Harris, N.B.W., Tindle, A.G., 1984, Trace element discrimination diagrams for the tectonic interpretation of granitic rocks: Journal of Petrology, 25, 956-983.

Peccerillo, A. Taylor, S.R., 1976, Geochemistry of Eocene calc-alkaline volcanic rocks from the Kastamonu area, northern Turkey: Contributions to Mineralogy and Petrology, 58, 63-81.

Roddick, J.C., Loveridge, W.D., Parrish, R.R., 1987, Precise U/Pb dating of zircons at the sub-nanogram Pb level: Chemical Geology, 66, 111-121.

Ruiz-Castellanos, M., 1979, Rubidium-strontium geochronology of the Oaxaca and Acatlán metamorphic areas of Southern Mexico: Dallas; Texas, University of Texas, Ph.D. Thesis, 188 p.

Ruíz, J., Patchett, P.J., Ortega-Gutiérrez, F., 1988, Proterozoic and Phanerozoic basement terranes of Mexico from Nd isotopic studies: Geological Society of America, Bulletin, 100, 274-281.

Sedlock, R.L., Ortega-Gutiérrez, F., Speed, R.C. (eds.), 1993, Tectonostratigraphic terranes and tectonic evolution of Mexico; Boulder, Colorado, Geological Society of America, Special Paper, núm. 278, 153 p.

Solari, L. A., Lopez, R., Cameron, K. L., Ortega-Gutiérrez, F., Keppie, J. D., 1998, Reconaissance U/Pb geochronology and common Pb isotopes from the northern portion of the 1Ga Oaxacan Complex, Southern Mexico: EOS, Transactions, American Geophysical Union, 79, p. F931. (abstract)

Sun, S.S., McDonough, W.F., 1989, Chemical and isotopic systematics of oceanic basalts–implications for mantle composition and processes, *in* Saunders, A.D., Norry, M.J. (eds.), Magmatism in the ocean basins: London, The Geological Society, Special Publication, 42, 313-345.

Tepley, F.J. III, Davidson, J.P., Tilling, R.I., Arth, J.G., 2000, Magma mixing, recharge and eruption histories recorded in plagioclase phenocrysts from El Chichón volcano, Mexico: Journal of Petrology, 41(9), 1,397-1,411.

Torres, R., Ruíz, J., Patchett, P.J., Grajales-Nishimura, J.M. 1999**,** Permo-Triassic continental arc in eastern Mexico; tectonic implications for reconstructions of southern North America, *in* Bartolini, C., Wilson, J.L., Lawton, T.F. (eds.), Mesozoic sedimentary and tectonic history of north-central Mexico: Boulder, Colorado, Geological Society of America, Special paper, 340, 191-196.

Weber, B., Kohler, H., 1999, Sm-Nd, Rb-Sr and U-Pb geochronology of a Grenville terrane in southern Mexico–origin and geologic history of the Guichicovi Complex: Precambrian Research, 96, 245-262.

Yáñez, P., Ruiz, J., Patchett, P.J., Ortega-Gutiérrez, F. Gehrels, G.E., 1991, Isotopic studies of the Acatlan Complex, southern Mexico–Implications for Paleozoic North American tectonics: Geological Society of America Bulletin, 103, 817-828.

Manuscript received: February 21, 2001.
Corrected manuscript received: June 18, 2001.
Manuscript accepted: June 18, 2001.